

ARTICLES

Disorder-induced roughening in the three-dimensional Ising model

M. J. Alava* and P. M. Duxbury

Department of Physics and Astronomy and Center for Fundamental Materials Research, Michigan State University, East Lansing, Michigan 48824

(Received 19 August 1996)

Using an exact method, we numerically study the zero-temperature roughness of interfaces in the random bond, cubic lattice, Ising model (of size L^3 , with $L \leq 80$). Interfaces oriented along the $\{100\}$ direction undergo a roughening transition from a weak disorder phase, which is almost flat, to a strong disorder phase with interface width $w \sim cL^{0.42}$ (c is a function of the disorder). For random dilution we find the roughening threshold $p_* = 0.89 \pm 0.01$ and $c \sim p_* - p$ for $p \leq p_*$ (p is the volume fraction of present bonds). In contrast $\{111\}$ interfaces are algebraically rough for all disorder. [S0163-1829(96)02845-7]

The statistical mechanics of interfaces in random media is a much-studied problem.¹⁻³ Physical realizations thereof include domain walls in Ising magnets,⁴⁻¹³ fracture, and yield surfaces in disordered materials^{14,15} and wetting problems.^{16,1} The fracture surface problem has in particular attracted a great deal of recent attention, with a continuing debate about whether the fracture surface exponents are controlled by disorder (minimal surfaces), by crack dynamics, or by a combination of the two.^{17,18} Here we calculate the roughness of minimal surfaces and hence show that, if disorder is dominant, then *the average orientation* of a fracture surface is important in the analysis of its roughness. This factor has not been assessed in the experiments so far.

In 1+1 dimensions, the random bond problem is related (through the Burgers' equation) to the celebrated Kardar-Parisi-Zhang (KPZ) model of kinetic growth.¹⁹ Although the 1+1 dimensional models (if d is the bulk dimension, we write $d_s + 1 = d$ where d_s is the surface dimension) have been intensely studied numerically, the more important 2+1 models have received little attention due to the numerical challenges involved in simulating *equilibrium* random surfaces in three dimensions (e.g., the usual problem with many metastable minima).^{20,21} Recently however,²² the use of the min-cut/max-flow algorithms from graph theory have made simulations of some 2+1 random surfaces relatively routine (these methods find the global minimum of this problem and avoid altogether getting stuck in metastable states). Here we use these methods to numerically study the *transition* from the weak disorder phase to the strong disorder phase in random magnets and minimal surfaces. We find that, for the 2+1 dimensional Ising model, this transition is at finite disorder for interfaces in the $\{100\}$ orientation, but is at zero disorder for interfaces in the $\{111\}$ orientation. In the $\{100\}$ case, the prefactor $c(p)$ (see the abstract) approaches zero continuously on approach to the transition.

Either disorder or thermal fluctuations immediately lead to roughening (i.e., $w \sim L^\zeta$, with $\zeta > 0$) in 1+1 dimensions. The roughening exponent in the thermal case $\zeta_T^{1+1} = 1/2$, while in the random-bond (RB) case we have the KPZ value

$\zeta_{RB}^{1+1} = 2/3$,⁶ and for random fields (RF) $\zeta_{RF}^{1+1} = 1$.^{4,5} In $d = d_s + 1$ dimensions, the random-field exponent appears to be consistent with the Imry-Ma argument^{4,5} $\zeta_{RF}^{d_s+1} = (4 - d_s)/3$, while for random bonds, the best results are from the functional renormalization group (RG) calculations, which give $\zeta_{RB}^{d_s+1} \sim b(4 - d_s)$, with $b = 0.2083$ (Ref. 10) (see also, Ref. 23). d_s is the surface dimension. Only recently has it been possible to test the $d_s > 1$ results to high precision.²² The current numerical result $\zeta_{RB}^{2+1} = 0.41 \pm 0.01$ is close to the RG result for random bonds and clearly distinct from the ($d_s = 2$) random-field exponent ($2/3$). These simulations²² were done for a $\{111\}$ orientation system, for a fixed continuous distribution of bond strengths, with the intent of numerically testing the predictions for ζ_{RB} . As we now show, when the disorder is varied, and in particular in the case of $\{100\}$ interfaces, there is a roughening threshold at finite disorder. That is, the exponents quoted above only apply for sufficiently strong disorder.

Consider a nearest-neighbor, random-bond Ising model on a cubic lattice, with Hamiltonian,

$$E = - \sum_{ij} J_{ij} s_i s_j, \quad (1)$$

where the spin variables have the values ± 1 . In the case of the diluted Ising model, bonds are present ($J_{ij} = 1$) with the probability p and absent ($J_{ij} = 0$) with probability $1 - p$. The spins on two opposite cube faces are aligned in opposite directions, forcing a domain wall somewhere in the middle of the system. The absent bonds act as local pins, and the surface reduces its energy by wandering to take advantage of these missing bonds. In the simple Imry-Ma arguments,^{4,5} one takes the energy cost of deforming the interface, $E_e \sim (w/L)^2 L^{d-1}$ (for a continuum) and compares it to the energy gain from the random bonds or fields. In the case of random fields $E_p^{RF} \sim (wL^{d-1})^{1/2}$, while a first approximation to the random-bond case is $E_p^{RB} \sim L^{(d-1)/2}$. The resulting "strong disorder" exponent is correct for random fields, but incorrect for random bonds (see the previous paragraph). For

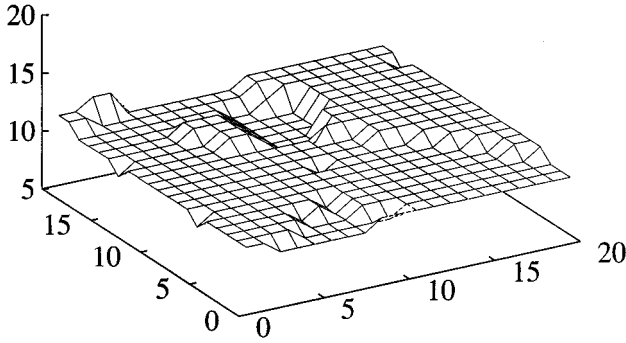


FIG. 1. $\{100\}$ interface in the diluted $L=20$, cubic lattice Ising model with $p=0.70$.

a $\{100\}$ Ising interface, the energy cost of deforming the interface can be higher than in the continuum due to lattice effects, so that $E_I \sim G_1(w/L)L^{d-1}$, where G_1 is a step-free energy. Comparing this energy with the random-bond and random-field energies, we find that for $d>3$, there is a flat phase at weak disorder. $d=3$ is the marginal dimension, and this suggests that in $d=3$, the interface width may scale logarithmically¹¹ for weak disorder. Note that in the $\{111\}$ direction the lattice effects are “washed out” by the high degeneracy of the ground-state interface of the pure system. In that case, we expect the “strong disorder” phase to apply for any finite disorder. Now we turn to direct numerical tests of the transition between the weak disorder phase and the strong disorder (algebraic) phase in the $\{100\}$ direction.

As described by Middleton,²² following related work by Ogielski²⁴ and work on critical current in high- T_c superconductors,²⁵ the interface problem in spin-1/2 ferromagnets with nearest-neighbor interactions is *exactly* the same as the min-cut/max-flow problem of operations research. In the latter problem one imagines injecting a flow, I , into a network whose bonds each have a different maximum allowed current (usually called a “capacity” in the operations research literature).²⁶ The problem is to find the “bottleneck” or cross section in the network which sets a limit on the amount of flow allowed through the system. This cross section is called the “minimum cut,” and once the “flow” capacity across it is saturated, “maximum-flow” is achieved. These problems are of vast importance in communications and transportation networks. In the diluted Ising system, the interface which minimizes the interface energy is the same as the min-cut. The interface energy is the maximum flow. The random-bond strengths map to the random capacities. The analogy fails if the magnetic model becomes a spin glass. The advantage of using this mapping is that the min-cut/max-flow problem can be solved exactly in polynomial time. We implemented a standard augmenting path algorithm^{25,26} to solve this problem, and with it we were able to find the *exact* minimum interface in a diluted Ising model of linear dimension L in polynomial time. For example for an 80^3 lattice at $p=0.9$, we found the exact lowest energy interface in 15 min using a 233 MHz DEC Alpha workstation. However, the algorithm scales as L^5 , so it is expensive at significantly larger system sizes. A “push-relabel” min-cut/max-flow algorithm is also available.^{27,22} The preliminary comparisons we have done between the two methods indicates that for this problem, the push-relabel method has

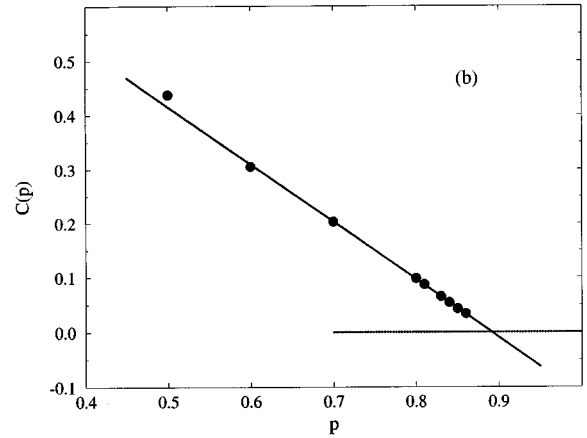
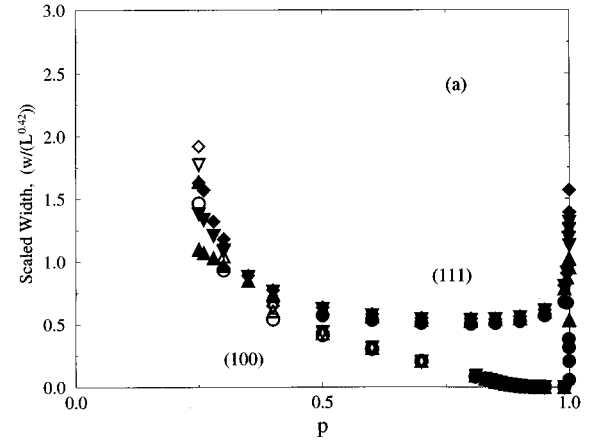


FIG. 2. Scaled interface width $w/L^{0.42}$ as a function of bond dilution p_1 with $J=1$. (a) Solid symbols are for $\{111\}$ interfaces, while open symbols are for $\{100\}$ interfaces. Calculations are for L (number of configurations)=10 (2000) {circles}, 20 (1500) {triangles}, 30 (1000) {inverted triangles}, 40 (200) {diamonds}. There is also data on $L=60$ (100 configurations) and $L=80$ (40 configurations) for $\{100\}$ interfaces near $p=0.90$, but the data collapse obscures the symbols on this plot. (b) A closer look at the value of p at which the $\{100\}$ scaled width approaches zero. The {solid circles} indicate data found by using a least-squares fit to the size-dependent widths and by assuming an exponent of 0.42 as found in (a). Using the solid line to extrapolate, we deduce that $p_* = 0.89 \pm 0.01$.

the better scaling behavior. Note that the min-cut/max-flow method is not restricted to “directed” surfaces, and so is able to find minimal energy interfaces which have overhangs. We calculated the interface width defined by, $w^2 = \langle h^2 \rangle - \langle h \rangle^2$ and the interface energy E and its fluctuations $\langle E^2 \rangle - \langle E \rangle^2$.

Figure 1 shows an example of the minimum energy configuration for an $L=20$, $\{100\}$ Ising interface. In Fig. 2, we present a scaled plot of the interface width ($w/L^{0.42}$) of such interfaces, where 0.42 is chosen to give the best data collapse. Thus, the strong disorder “minimal surface” exponent in 2+1 dimensions is 0.42 ± 0.02 in agreement with RG calculations^{10,21} and with numerical simulations.²² For the $\{100\}$ case [triangles in Fig. 2(a)], there is a threshold above which the scaled interface width is zero. An analysis of this threshold behavior is presented in Fig. 2(b). The solid dots

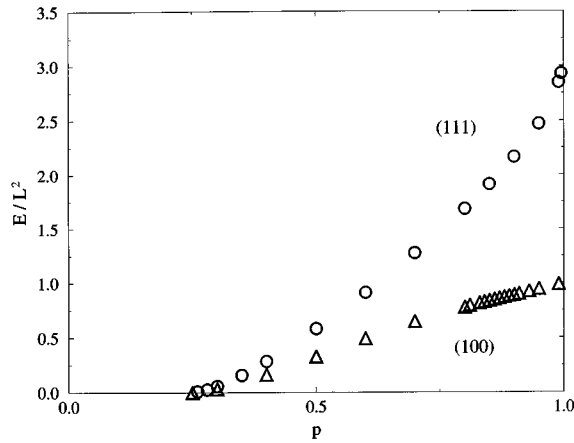


FIG. 3. The interface energy of the diluted 3d Ising model. The values plotted are found by extrapolation using the same simulation data as those used in Fig. 2(a). Triangles are for the {111} orientation, while circles are for the {100} case.

are found from a least-squares fit to the size-dependent widths, assuming the minimal surface exponent 0.42 as found in Fig. 2(a). It is seen from this figure that for $p_c \ll p < p_*$, $w \sim c(p)L^{0.42}$, with $c(p) \sim p_* - p$ and $p_* = 0.89 \pm 0.01$. At smaller p , the scaled width increases and in fact, $w/L^{0.42}$ diverges on approach to the percolation threshold p_c [see Fig. 2(a)]. This is expected because at p_c , $w \sim L$ due to the isotropic fractal character of the infinite cluster. We also assessed whether the data may indicate a continuously varying exponent rather than the threshold behavior extracted above. However if we fit the data in that way, there is a sharp transition in the “effective exponent” near $p_* = 0.89$. Note that the interfaces studied here scale in a manner consistent with conventional scaling in contrast to recent suggestions that there may be a breakdown of scaling in the bulk properties of the 3d diluted Ising model.²⁸ Finally there is another replica-type continuum field theory²⁹ which indicates that {100} interfaces remain strongly disordered for all p , but that one must go to length scales $L \gg L_c \sim \exp(1/\alpha)$ in order to reach the strong disorder regime. Here α is a disorder parameter which approaches zero as $p \rightarrow 1$. Questions remain about whether this result is relevant to the lattice interfaces studied here.

In the {111} direction [see Fig. 2(a), solid symbols], there is no threshold behavior at finite p , and the divergence at p_c still occurs. However there is an additional interesting behavior very close to $p = 1$. To understand this effect, consider the many degenerate interface configurations which occur in a {111} interface at $p = 1$. Now imagine putting one defect in the lattice. This selects from the degenerate set those which pass through the defect. Now add two defects to the lattice. This selects from the ground-state ensemble of “pure limit” interfaces those which have a roughness which is roughly proportional to the vertical separation between the two defects. Since the two defects are equally likely to be separated by distances in the interval $(0, L)$, the average roughness scales as L . Thus there is a singular behavior near the pure limit for the {111} interface. Note however, that once the deviation from the pure limit $1 - p > 1/L^{0.42}$, the pure limit ground-state ensemble is no longer relevant, and the behavior returns to the strong disorder minimal surface behavior.

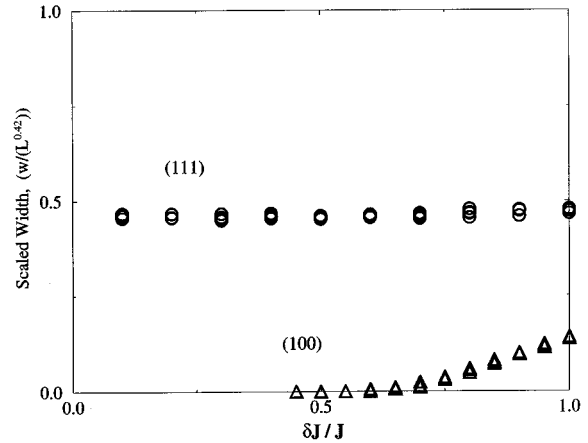


FIG. 4. A plot of the scaled width of interfaces in the 3d random bond Ising model with bond couplings drawn from a distribution of mean $J=1$ and half-width δJ . The {111} data is for lattices of size $L=10,20,30,40$, while the {100} data is for lattices of size $L=10,20,30$.

As is expected, the interface energy E is smooth for all p (see Fig. 3) and approaches zero as $p \rightarrow p_c$. That is, over the entire range $p > p_c$, the leading term in the interface energy scales as $E = a(p)L^{d_s}$. In the pure limit ($p=1$) $a(p)=3$ for the {111} orientation and $a(p)=1$ for the {100} orientation, as expected. However, there are singular corrections to the interface energy, so that $E \sim a(p)L^{d_s} + b(p)L^\theta$. The interface energy fluctuations $\langle E^2 \rangle - \langle E \rangle^2$ are also controlled by the exponent θ , and we find, $\langle E^2 \rangle - \langle E \rangle^2 \sim L^{2\theta}$ with $\theta = 0.82 \pm 0.05$ for $p_c < p < p_*$. This is consistent with the scaling hypothesis $\theta = 2\zeta$.

The presence of the roughening threshold for the {100} orientation is not peculiar to the case of random dilution. For example, a uniform distribution centered at J and with width $2\delta J$ also shows this effect (see Fig. 4, triangles). Again in the rough phase, the scaling exponent is 0.42 ± 0.01 . In this case, for the sample sizes studied, the surface is *completely* flat for $\delta J < 0.5$. The case $\delta J = 1$ corresponds to the distribution extending to the origin. In the {111} orientation (circles in Fig. 4), the roughness exponent 0.42 applies for all values of δJ . The anomalous behavior seen near the pure limit in the case of random dilution does not occur for the continuous distribution.

In summary, $T=0$ interfaces in cubic lattice Ising models exhibit a disorder-induced roughening transition for the {100} orientation. The transition is between a weak disorder “almost flat” phase and a strong disorder phase which has width $w \sim L^{0.42}$. In contrast in the {111} orientation, the interface is always strongly disordered. This has direct implications for recent measurements^{14,15,17,18} of the roughness of fracture surfaces, where “quasistatic” cleavage along the {100} orientation could have different roughness than fracture occurring at other orientations, at least for weakly disordered materials.

This work has been supported by DOE Grant No. DE-FG02-090-ER45418 and by the Academy of Finland (M.J.A.). P.M.D. thanks A. Bovier, E. Bouchaud, J. P. Bouchaud, and W. Selke for useful electronic mail correspondence.

- *Permanent address: Laboratory of Physics, Helsinki University of Technology, Espoo, Finland.
- ¹G. Forgacs, R. Lipowsky, and Th. M. Nieuwenhuizen, in *Phase Transitions and Critical Phenomena*, edited by C. Domb and J. L. Lebowitz (Academic, San Diego, 1991), Vol. 14.
 - ²A.-L. Barabási and H. E. Stanley, *Fractal Concepts in Surface Growth* (Cambridge University Press, Cambridge, 1995).
 - ³T. Halpin-Healy and Y.-C. Zhang, *Phys. Rep.* **254**, 215 (1995).
 - ⁴Y. Imry and S.-K. Ma, *Phys. Rev. Lett.* **35**, 1399 (1975).
 - ⁵G. Grinstein and S. K. Ma, *Phys. Rev. B* **38**, 2588 (1983).
 - ⁶D. A. Huse and C. L. Henley, *Phys. Rev. Lett.* **54**, 2708 (1985).
 - ⁷D. A. Huse, C. L. Henley, and D. Fisher, *Phys. Rev. Lett.* **55**, 2924 (1985).
 - ⁸M. Kardar, *Phys. Rev. Lett.* **55**, 2235 (1985).
 - ⁹M. Kardar, *Phys. Rev. Lett.* **55**, 2923 (1985).
 - ¹⁰D. Fisher, *Phys. Rev. Lett.* **56**, 1964 (1986).
 - ¹¹A. Bovier, J. Frölich, and U. Glaus, *Phys. Rev. B* **34**, 6409 (1986).
 - ¹²T. Nattermann and I. Vilfan, *Phys. Rev. Lett.* **61**, 223 (1988).
 - ¹³A. Bovier and C. Külske, *Rev. Math. Phys.* **6**, 413 (1994); A. Bovier and C. Külske (unpublished).
 - ¹⁴E. Bouchaud and J. P. Bouchaud, *Phys. Rev. B* **50**, 17 752 (1994); P. Daguier, S. Henaux, E. Bouchaud, and F. Creuzet (unpublished).
 - ¹⁵S. Roux and A. Hansen, *J. Phys. (France) III* **2**, 1007 (1992).
 - ¹⁶M. Huang, M. E. Fisher, and R. Lipowsky, *Phys. Rev. B* **39**, 2632 (1989).
 - ¹⁷V. Y. Milman, N. A. Stelmashenko, and R. Blumenfeld, *Prog. Mater. Sci.* **38**, 425 (1994).
 - ¹⁸E. Bouchard and S. Navéos, *J. Phys. (France) I* **5**, 547 (1995).
 - ¹⁹M. Kardar, G. Parisi, and Y.-C. Zhang, *Phys. Rev. Lett.* **56**, 889 (1986).
 - ²⁰M. Kardar and Y.-C. Zhang, *Europhys. Lett.* **8**, 232 (1989).
 - ²¹Z. Jiang and C. Ebner, *Phys. Rev. B* **41**, 9121 (1990).
 - ²²A. A. Middleton, *Phys. Rev. E* **52**, R3337 (1995).
 - ²³T. Halpin-Healy, *Phys. Rev. B* **42**, 711 (1990).
 - ²⁴T. T. Ogielski, *Phys. Rev. Lett.* **57**, 1251 (1986).
 - ²⁵R. Riedinger, *Cryogenics* **30**, 465 (1990).
 - ²⁶L. R. Ford and D. R. Fulkerson, *Flows in Networks* (Princeton University Press, Princeton, NJ, 1962). See also any standard book on graph theory and flow problems.
 - ²⁷A. V. Goldberg and R. E. Tarjan, *J. Assoc. Comput. Mach.* **35**, 921 (1988).
 - ²⁸V. Dotsenko, A. B. Harris, D. Sherrington, and R. B. Stinchcombe, *J. Phys. A* **28**, 3093 (1995).
 - ²⁹J. P. Bouchard and A. Georges, *Phys. Rev. Lett.* **68**, 3908 (1992).